On the Provenance of Hinged-Hinged Frequencies in Timoshenko Beam Theory

W.P. Howson[1] and A. Watson[2]

[1] Independent Consultant, Gwanwyn, Craig Penlline, CF71 7RT, UK

[2] Corresponding Author

Department of Aeronautical and Automotive Engineering, Loughborough University, UK

C & S PAPER
061117

FINAL REVISED VERSION

Contact information

ABSTRACT

An exact differential equation governing the motion of an axially loaded Timoshenko beam supported on a two parameter, distributed foundation is presented. Attention is initially focused on establishing the provenance of those Timoshenko frequencies generated from the hinged-hinged case, both with and without the foundation being present. The latter option then enables an exact, neo-classical assessment of the 'so called' two frequency spectra, together with their corresponding modal vectors, to be undertaken when zero, tensile or compressive static axial loads are present in the member. An alternative, 'precise' approach, that models Timoshenko theory efficiently, but eliminates the possibility of a second spectrum, is then described and used to confirm the original eigenvalues. This leads to a definitive conclusion regarding the structure of the Timoshenko spectrum. The 'precise' technique is subsequently extended to allow, either the full foundation to be incorporated, or either of its component parts individually. An illustrative example from the literature is solved to confirm the accuracy of the approach, the nature of the Timoshenko spectrum and a wider indication of the effects that a distributed foundation can have.

1. Introduction

A knowledge of the vibration of beams and beam systems is a modern requirement across a diverse range of engineering and scientific disciplines, no better typified than in the aerospace industry. Of the vibration theories available, Bernoulli-Euler theory is the simplest and most widely understood. It underpins the majority of practical applications, which involve members with moderate to high slenderness ratios, but requires modification when the members carry a static axial force of significant value. In similar fashion, when members have a low slenderness ratio or vibrate at high frequency, the second order effects of rotary inertia of the cross-section and shear deformation must be taken into account; the so-called Timoshenko theory.

Since its inception in 1921 [1], Timoshenko beam theory has generated an almost relentless flow of research on virtually every aspect of its sphere of influence. Despite this, there are still a surprising number of topics that can benefit from further attention and subsequent explanation. One of these concerns the provenance of frequencies determined through Timoshenko beam theory. Unlike Bernoulli-Euler theory, which is well understood for single members, there has long been conjecture regarding a particular aspect of Timoshenko theory, namely the point discontinuity in the governing differential equation and the subsequent division of frequencies into two spectra. Background to this area of work can be found, for example, in the following papers [2-9], which themselves contain a wide variety of references.

In the work that follows, a unified, exact member theory that incorporates all the second order effects of static axial load, rotary inertia and shear deformation is presented in a way that enables a critical assessment to be made of the point discontinuity in the Timoshenko equation. This leads to a clarification of the status of the corresponding cut-off frequency, which in turn enables a definitive conclusion to be drawn about the Timoshenko spectrum. The evidence thus gathered is further used to cast light on the corresponding modal vectors and other related topics of interest.

Initially, the exact differential equation governing the motion of a Timoshenko beam supported on a two parameter, distributed foundation is presented in a convenient, non-dimensional form that allows for the possibility of a zero, tensile or compressive static axial load in the member. The basic hinged-hinged relationships required in the remainder of the paper are then developed concisely, in such a way that shows how the continuous spectrum of Bernoulli-Euler (B-E) frequencies are related to their Timoshenko counterparts. The paper then focuses in more detail on the case of an axially loaded, hinged-hinged Timoshenko beam in the absence of an elastic foundation. It is shown how the frequency equation factorizes, the nature of the second spectrum is discussed, together with its influence on mode shape recovery, and a simple, physical comparison is made between any combination of hinged and guided boundary conditions.

A 'precise' approach for converging upon any required Timoshenko frequency in an extremely efficient way, is then described. In the absence of a distributed foundation, this involves establishing a stiffness

matrix using Bernoulli-Euler theory that allows exactly for static axial load and shear deformation and then augmenting it with a close approximation to the distributed rotational inertia. Such an approach eliminates the possibility of a second spectrum and when used in conjunction with the Wittrick-Williams algorithm [10], ensures convergence to any required natural frequency with the certain knowledge that none have been missed. This theory is subsequently used to confirm the exact results from the corresponding equations presented earlier, by mapping the step-by-step transformation of the B-E frequencies to their equivalent Timoshenko values. This process underlines the need to reassess the discontinuity in the Timoshenko equation and hence the status of the cut-off frequency.

Attention is then focused on establishing the corresponding eigenvalues when the member is supported on a two-parameter, distributed foundation. Exact solution of the Timoshenko problem in such cases has been considered previously by Capron and Williams [11] and has been shown to be intractable. In contrast, it is shown herein that equivalent solutions to the hinged-hinged case, can be generated through the 'precise' approach, to good accuracy, by implementing a minor modification, and furthermore, that extension to any possible combination of elastic end conditions is equally straightforward. An additional point of note that emerges from the above is that, for the hinged-hinged case, two possible discontinuities in the governing differential equation can now be identified.

Finally, the theory of this paper is applied to a well-known, illustrative problem, from which a number of conclusions are drawn and recommendations made.

2. Theory

An exact, fourth order differential equation governing the motion of an axially loaded Timoshenko beam of length, L, that is supported on a two parameter, distributed foundation, whose lateral and rotational restraining stiffnesses per unit length are k_y and k_θ, respectively, has been given by Capron and Williams [11] and can be written in the following non-dimensional form

$$[D^4 + 2(\Delta - k_1^*)D^2 - (qb^2 - k_2^*)/t]\Theta = 0 \tag{1}$$

where $D = d/d\xi$, $\xi = x/L$ is the non-dimensional length parameter and $\Theta = V$ or Ψ, where V and Ψ are the amplitudes of the lateral displacement and bending slope, respectively.

$$\Delta = [qp^2 + b^2(r^2 + s^2)]/2t \qquad q = 1 - b^2 r^2 s^2 \qquad b^2 = \rho A L^4 \omega^2 / EI \qquad t = 1 - s^2 p^2 \tag{2a}$$

$$k_1^* = (s^2 k_y^* + t k_\theta^*)/2t \qquad k_2^* = q k_y^* - s^2 k_\theta^* (b^2 - k_y^*) \tag{2b}$$

$$p^2 = PL^2/EI \qquad r^2 = I/AL^2 \qquad s^2 = EI/\kappa AGL^2 \qquad k_y^* = k_y L^4/EI \qquad k_\theta^* = k_\theta L^2/EI \tag{2c}$$

where ρ, E and G are the density, Young's modulus and shear modulus of the member material respectively, A and I are the area and second moment of area of the cross-section, κ is the section shape factor, ω is the radian frequency of vibration and P is the static axial load in the member, which is positive for compression, zero, or negative for tension. The non-dimensional parameters b^2, p^2, r^2 and s^2 uniquely define the effects of frequency, axial load, rotary inertia and shear deformation, respectively [12,13]. For generality, the work that follows is developed in terms of b and b^2 which, for conciseness, are merely referred to as frequencies, while any combination of the remaining effects can be neglected by setting the relevant parameter to zero. Finally, it can be demonstrated that, t, defined by the last of Eqs.(2a), is always positive so long as P is less than the elastic critical buckling load (when in compression and does not cause inelastic behaviour when in tension.

2.1. Frequency relationships for the hinged-hinged case

For this case, it is convenient to consider Eq.(1) with $\Theta = V$ and to assume a general solution of the form $V = C\sin i\pi\xi$, where C is an arbitrary constant and V satisfies the boundary conditions. Substituting for V in Eq.(1) then yields

$$(i\pi)^4 - 2(\Delta_i - k_1^*)(i\pi)^2 - (q_i b_i^2 - k_2^*)/t = 0 \qquad i = 1,2,....\infty \tag{3}$$

Eq.(3) can now be used to find any frequency, b_i, for any combination of the non-dimensional parameters defined in Eqs.(2). However, for the context of this paper, it is first necessary to consider the simple B-E beam, for which $p^2 = r^2 = s^2 = k_y^* = k_\theta^* = 0$. Substituting these parameters in Eq.(3) yields the i^{th} B-E frequency, $b_{0,i}$, as

$$b_{0,i} = (i\pi)^2 \qquad i = 1,2,....\infty \tag{4}$$

Attention is now focused on relating the i^{th} B-E frequency to its counterparts emanating from any desired combination of non-dimensional parameters. This is most easily achieved by embedding Eq.(4) into Eq.(3), to yield

$$(1 - s^2p^2)b_{0,i}^2 - \{p^2 + (b_i^2r^2 - k_\theta^*)(1 - s^2p^2) + s^2(b_i^2 - k_y^*)\}b_{0,i}$$

$$-(b_i^2 - k_y^*)\{1 - s^2(b_i^2r^2 - k_\theta^*)\} = 0 \qquad i = 1,2,....\infty \tag{5}$$

which, upon expansion, yields the quadratic frequency equation in the non-dimensional frequency parameter, b_i^2, as

$$b_i^4r^2s^2 - \{1 + [r^2(1 - s^2p^2) + s^2]b_{0,i} + s^2(r^2k_y^* + k_\theta^*)\}b_i^2$$

$$+(1 - s^2p^2)b_{0,i}^2 - [p^2 - s^2k_y^* - (1 - s^2p^2)k_\theta^*]b_{0,i} + (1 + s^2k_\theta^*)k_y^* = 0 \qquad i = 1,2,....\infty \tag{6}$$

A further closed form relationship of interest can be established by ignoring the effects of rotary inertia, i.e. setting $r^2 = 0$ in Eq.(6), to yield

$$b_{psy\theta,i}^2 = \{(1 - s^2p^2)b_{0,i}^2 - [p^2 - (1 - s^2p^2)k_\theta^* - s^2k_y^*]b_{0,i} + (1 + s^2k_\theta^*)k_y^*\}$$

$$/[1 + s^2(b_{0,i} + k_\theta^*)] \qquad i = 1,2,....\infty \tag{7}$$

where the lowercase subscripts on the left hand side of the equation, other than *i*, denote the non-dimensional parameter(s) retained.

2.2. Equivalent equations in the absence of a distributed foundation

The effects of a two parameter foundation can be eliminated simply from Eqs.(1), (5), (6) and (7) by setting $k_y^* = k_\theta^* = 0$ to yield

$$[D^4 + 2\Delta D^2 - qb^2/t]\,\Theta = 0 \tag{8}$$

$$(1 - s^2p^2)b_{0,i}^2 - \{p^2 + b_i^2r^2(1 - s^2p^2) + b_i^2s^2\}b_{0,i} - b_i^2(1 - b_i^2r^2s^2) = 0 \qquad i = 1,2,....\infty \tag{9}$$

$$b_i^4r^2s^2 - \{1 + [r^2(1 - s^2p^2) + s^2]b_{0,i}\}b_i^2 + (1 - s^2p^2)b_{0,i}^2 - p^2b_{0,i} = 0 \qquad i = 1,2,....\infty \tag{10}$$

$$b_{ps,i}^2 = \{(1 - s^2p^2)b_{0,i}^2 - p^2b_{0,i}\}/(1 + s^2b_{0,i}) \qquad i = 1,2,....\infty \tag{11}$$

respectively.

Solutions to Eq.(8) can now be found easily, for any required combination of boundary conditions, using the dynamic stiffness technique in conjunction with the Wittrick-Williams algorithm, as described in detail in references [12,13]. Since such solutions are founded in exact member theory and can be converged upon to the accuracy of the host computer, the accuracy of such results is commensurate with that of closed form solutions.

Eq.(8) yields Eq.(9) exactly for the case of hinged-hinged boundary conditions which, on expansion, yields the quadratic equation in b_i^2 that is given in Eq.(10). Thus either equation can be used to generate the required frequency parameters, the former by trial values of b_i and the latter from a classical route.

Finally, it is clear that Eqs.(7) and (11) are simple, exact closed form solutions and are typical of a family of such equations formed from various combinations of the non-dimensional parameters, in which either r^2, s^2 or both are zero. In both equations presented, the effects of axial load and shear deformation are accounted for exactly, while the effects of rotary inertia are ignored. Once more it is straightforward to show that the right hand side of Eq.(11) is always positive, with the result that each frequency generated is related uniquely to a single B-E frequency, which thus forms part of a single continuous spectrum. Such an argument must also hold for Eq.(7), since adding stiffness to a structure cannot reduce the values of its natural frequencies. Furthermore, it is a requirement of any theory that seeks to improve the accuracy of B-E theory, that each frequency is modified without loss or addition of any frequencies. This is clearly satisfied by Eqs.(7), (11) and all similar equations that constitute the family.

In contrast, Eq.(10) shows that although the complete spectrum of Timoshenko frequencies can be determined through an entirely consistent approach, each pair of frequencies now stems from a single B-E frequency and hence the one-to-one relationship between a developed frequency and a unique B-E frequency appears to have been lost.

Consider therefore the lower and upper solutions to Eq.(10), which can be written as, respectively,

$$b_{L,i}^2 = (\alpha_i - \beta_i^{1/2})/2r^2s^2 \quad \text{and} \quad b_{U,i}^2 = (\alpha_i + \beta_i^{1/2})/2r^2s^2 \tag{12a,b}$$

where

$$\alpha_i = 1 + b_{0,i}[r^2(1-s^2p^2) + s^2] \quad \text{and} \quad \beta_i = \alpha_i^2 - 4r^2s^2b_{0,i}[b_{0,i}(1-s^2p^2) - p^2] \tag{13a,b}$$

It is then straightforward to show that β_i, the discriminant of Eq.(10), is always positive and that both roots are also positive, subject to the constraints imposed earlier on *P*.

2.3. The two frequency spectra

Timoshenko beam theory, as defined by Eq.(8), has a discontinuity when

$$q = 1 - b^2r^2s^2 = 0 \quad \text{i.e. when} \quad b_{co}^2 = 1/r^2s^2 \tag{14a,b}$$

where b_{co}^2 defines the cut-off frequency. Beyond this point, the natural frequencies stem from two sources, the first (original) spectrum and the 'so-called' second spectrum, as discussed later in this section.

Before that, it is important to deal with the lack of clarity surrounding the cut-off frequency, which lies at the heart of the current debate on this aspect of Timoshenko theory. The problem stems from the fact that the cut-off frequency corresponds to the point discontinuity in the Timoshenko equation and as such has never been ascribed any intrinsic value, over and above defining the lower limit of the second spectrum. However, there are a number of indications that this should not be so. For example, the cut-off frequency can be captured using Timoshenko theory, since Eq.(8) is valid in the range $0 < 1 - b^2r^2s^2 < 0$ and therefore offers the possibility of infinitely close upper and lower bounds on the cut-off frequency, subject only to the accuracy of the host computer. i.e. the accuracy to which any other frequency can be converged upon. Furthermore, it can be shown that the cut-off frequency and its mode shape correspond

exactly to the lowest frequency and mode shape of an infinite family of pure shear modes that are governed by a second order differential equation [2]. Since the pure shear mode corresponding to the cut-off frequency is clearly a possible mode of a hinged-hinged member, it implies that the determinant in a transcendental dynamic stiffness approach must change sign through zero rather than infinity. Thus any theory, exact or approximate, that seeks to converge on Timoshenko frequencies can include the cut-off frequency in its spectrum by ensuring that its root count algorithm increases by one as the trial frequency passes through the cut-off frequency. Finally, it is shown in Section 3 that there is always a Bernoulli-Euler frequency that maps to the cut-off frequency. The implications stemming from the above points are discussed later in Sections 4 and 5.

The factorisation of the hinged-hinged frequency equation, which leads to the two frequency spectra of Timoshenko beam theory, has been dealt with by a number of authors, as alluded to in the Introduction. Stephen [8] has also described the extensions necessary to include the related cases of guided-guided and hinged-guided boundary conditions. However, there are also some simple physical relationships that exist between these boundary conditions that are of interest and these are presented in the Appendix.

In order to facilitate further comparison, it is necessary to establish the manner in which Eq.(8) factorises in the case of a hinged-hinged member to yield the two spectra of Timoshenko frequencies. This is described in detail in [12] and in outline below. Thus from [12], and with the current notation, the required natural frequencies correspond to

$$\sin \Phi_i = 0 \qquad \text{when} \qquad q_i > 0 \qquad\qquad i = 1,2,....\infty \tag{15a}$$

and

$$\sin \Phi_i \sin \Lambda_i = 0 \qquad \text{when} \qquad q_i < 0 \qquad\qquad i = 1,2,....\infty \tag{15b}$$

where

$$\Phi_i^2 = \Delta_i + (\Delta_i^2 + q_i b_i^2 / t)^{1/2} \qquad \text{and} \qquad \Lambda_i^2 = \Delta_i - (\Delta_i^2 + q_i b_i^2 / t)^{1/2} \tag{16a,b}$$

and the right hand sides of Eqs.(16) are defined by Eqs.(2). The frequencies, $b_{\Phi,i}$, corresponding to $\sin \Phi_i = 0$ constitute the first spectrum, while those frequencies, $b_{\Lambda,i}$, corresponding to $\sin \Lambda_i = 0$ constitute the second. The frequencies in the first and second spectrum can therefore be found from, Eqs.(16) by substituting, respectively,

$$\Phi_i = i\pi \qquad \text{and} \qquad \Lambda_i = i\pi \qquad\qquad i = 1,2,....\infty \tag{17a,b}$$

The frequencies $b_{\Phi,i}$ and $b_{\Lambda,i}$ are evidently the solutions of Eq.(9) and hence of Eq.(10). They must therefore be identical to the solutions of Eq.(10) that stem from Eqs.(12), with the result that

$$b_{\Phi,i} = b_{L,i} \qquad \text{and} \qquad b_{\Lambda,i} = b_{U,i} \tag{18a,b}$$

2.3.1. Mode shape retrieval and interpretation

The mode shapes corresponding to those frequencies obtained through Timoshenko theory are straightforward to develop by any appropriate method. In the current context of converging on the required frequencies using a stiffness formulation and the Wittrick-Williams algorithm [10], the method of mode extraction used is described in detail by Hopper and Williams [14] and implemented in the computer program described in [13]. The mode shape corresponding to the cut-off frequency is the only possible pure shear mode and is easy to recognise, since the lateral displacement is zero and the bending slope is a constant value along the length of the member. Hence the modal number is either known by inspection or can be calculated *a priori* through Eq.(21). All other modes are flexural with those below the cut-off frequency stemming from the first spectrum and those above the cut-off frequency stemming from either. For those modes occurring above the cut-off frequency, it is helpful to identify their origin

either from Eqs.(12) or (16) and these will be designated Φ_m and Λ_n modes, corresponding to the first and second spectrum, respectively. Since the modes are functions of sine terms and the member has hinged-hinged supports, all modes will have *m* or *n* half sine waves along the full length of the member and the lateral displacement will be either symmetric or antisymmetric about its mid-length depending on whether *m* or *n* is odd or even, respectively, with the corresponding rotational displacement being out of phase by $3\pi/2$ for Φ_m modes and $\pi/2$ for Λ_n modes. This is due to the fact that the sign of the shear slope and the sign of the bending slope can be shown to be the same for the Φ_m modes and opposite for the Λ_n modes [15]. It also confirms that the corresponding Φ_m and Λ_n modes, in which $m = n$, satisfy the necessary condition of independence between themselves and every other mode. These points are further clarified in Tables 4 and 5 and Figs. 1 and 2, which highlight a selection of mode shapes stemming from the results of the Numerical Example of Section 3.

2.4. A 'precise' approach

In the 'precise' approach used herein, the original uniform member of length, *L*, is notionally divided into *NS* segments of equal length, *LS*, such that

$$NS = 2^M \quad \text{and} \quad LS = L / NS \tag{19a,b}$$

where *M* is an integer that ultimately defines the numerical accuracy of the solution. An 'appropriate' dynamic stiffness matrix is then formulated for a single datum segment of length *LS*, using a theory that reflects, as accurately as possible, the behaviour of the original member, but which lends itself to simpler solution. The first step is then to determine the number of clamped ended frequencies of the datum segment that have been passed by the trial frequency. An approximation to the original member is then reconstituted from the datum segment in *M* doubling procedures. In the first of these, two datum segments are joined together end to end to form a new segment of length $2 \times LS$. This implies the addition of two datum stiffness matrices followed by Gauss elimination to eliminate the central node. This is also a necessary step in the Wittrick-Williams algorithm [10] for accumulating the number of natural frequencies passed by the trial frequency. This doubling procedure is then used recursively [16-18] a further $M - 1$ times, until an approximation to the original member has been formed in terms of its dynamic stiffness matrix. Once this has been achieved, the boundary conditions are imposed on the resulting stiffness matrix and the Wittrick-Williams root counting algorithm [10] is completed by establishing the 'sign count' of the final matrix *i.e.* the number of negative leading diagonal elements of the matrix following Gauss elimination in its standard form. Iterative use of this process enables convergence upon the currently required natural frequency, and subsequently on all required natural frequencies to any desired accuracy with the certain knowledge that none have been missed.

2.4.1. The hinged-hinged case in the absence of a distributed foundation

In this case, the 'appropriate' datum stiffness matrix is developed using exact B-E theory with exact allowance for axial load and shear deformation. *i.e.* the dynamic stiffness equivalent of Eq.(11) that clearly has a single, continuous frequency spectrum. The distributed rotary inertia of the datum segment is then calculated and half is allocated as a lumped inertia to each of the direct rotational stiffness locations of the datum stiffness matrix. The member is then reconstituted from the datum matrix in the way described above, with the result that an equivalent Timoshenko member has been formed through a route that has eliminated the possibility of a second spectrum. It can be seen that the 'precise' results presented for the numerical example of Section 3 show exceptionally good accuracy when compared to the equivalent exact results.

2.4.2. The hinged-hinged case in the presence of a distributed foundation

The relatively simple boundary conditions of this case enable Eq.(1) to be written in the form of Eq.(5) and subsequently Eq.(6). However, the difficulties in solving Eq.(1) exactly, are also apparent in Eq.(6), where the discriminant of the quadratic equation can be awkwardly volatile and difficult to deal with. Thus it is useful to adopt once more the approach described in Section 2.4.1 above, but this time based on Eq.(7). This presents a more difficult problem than previously, until it is noted that Eq.(11) is Eq.(7) with the foundation stiffnesses removed. It is then a simple matter to use the original datum segment matrix, but now augmented with lumped stiffnesses, equivalent to the original distributed foundation stiffnesses, which are divided equally between the appropriate direct stiffness locations at each end of the datum segment. The process of reconstitution is then undertaken as before.

Finally, it is interesting to note from either Eq.(1) or Eq.(5), that there now appears to be two possible discontinuities, namely at

$$b_i^2 = (1 + s^2 k_\theta^*)/r^2 s^2 \quad \text{and} \quad b_i^2 = k_y^* \tag{20a,b}$$

The first is a variation of the original cut-off frequency, modified solely by the rotational component of foundation stiffness, which therefore maintains its identity as a pure shear mode, while the second is a function of the lateral foundation stiffness only. In the 'precise' approach proposed herein, the substitution of approximate lumped foundation stiffnesses to replace the original distributed stiffnesses, relegates the root counting procedures necessary to account for Eqs.(20), to the purely mechanical task of establishing the 'sign count' of the reconstituted, dynamic member stiffness matrix, as discussed in Section 2.4.2. In contrast, the complexities imposed by these discontinuities in an exact environment have been discussed in detail by Capron and Williams [11].

2.4.3. The 'precise' solution of Eq.(1) with any combination of elastic end conditions

It should be noted that the problem described in Section 2.4.2 requires no specific knowledge of Eq.(1), but only the datum segment matrix of the equivalent Timoshenko beam developed in Section 2.4.1 and its augmentation with equivalent foundation stiffnesses in Section 2.4.2. Thus the only difference between the hinged-hinged case and this one, is the imposition of any combination of nodal elastic boundary conditions at the end of each iteration of the Wittrick-Williams process and their subsequent effect on the 'sign count', as discussed in Section 2.4.

3. Numerical example

The problem of a hinged-hinged Timoshenko beam, originally solved by Levinson and Cooke [5] and extended by Stephen [8] is now considered in a variety of ways. The basic member data are as follows. Young's modulus $E = 210$ GN/m^2, density $\rho =$ 7850 kg/m^3, Poisson's ratio $\nu =$ 0.3, the shear coefficient $\kappa = 5(1+\nu)/(6+5\nu)$, length $L = 0.5$m, depth $d =$ 0.125m and breadth equal to unity. The axial load in the member when not zero is ± 0.675 GN, which is approximately half its Euler load when in compression.

4. Results and discussion

The results emanating from the analysis of the above data are presented in Tables 1 to 7 and Figs. 1 and 2. In each of Tables 1 to 3 and 6 to 7, the columns are numbered to facilitate description and the core results forming the body of the table are the required non-dimensional frequency values, b_i. Each table is divided into three sections, depending on whether the axial load is zero, tensile or compressive. The results in the tensile and compressive sections follow the results for the unloaded member in a predictable way and create no anomalies. The descriptions given thus relate to all three sections of the tables. Tables 4 and 5 are structured differently and together with Figs. 1 and 2 describe the attributes of a selection of mode shapes that typify the motion over the range of frequencies examined.

Table 1 lists the non-dimensional frequency parameters, b_i, stemming from Eq.(11) with $s^2 = 0$ (columns 2, 4 and 6) and $s^2 \neq 0$ (columns 3, 5 and 7). Consider first the odd numbered columns. It is

clear that each of these results, which allow exactly for the effects of axial load and shear deformation in the member, but make no allowance for rotary inertia, bare a unique relationship to their corresponding B-E frequencies. These results therefore constitute part of an infinite, unbroken single spectrum of frequencies. In contrast, the equivalent Timoshenko frequencies listed in Table 2 are generated in pairs, being the lower and upper solutions of Eq.(10), the governing quadratic equation, which is seeded by a single value. Thus the notion that a single B-E frequency is uniquely related to a single Timoshenko frequency appears to be unfounded. In turn, this throws doubt on a theory that purports to improve the accuracy of all frequencies stemming from the simpler B-E model.

Table 3 compares results from a number of equations in the body of the paper, together with additional supporting information. The exact results in column 2 are generated from Eq.(11) with $s^2 \neq 0$ and provide an upper bound datum for the remainder of the frequencies shown in the table. The results from the 'precise' approach, which is described in Section 2.4, are presented in columns 3-6 and correspond to the number of doubling procedures undertaken in each case. M = 3 indicates that the reconstituted member would be modelled by eight segments. In contrast, $M = 12$ indicates that it would be modelled by 4096 segments in only twelve doubling procedures. In the latter case, the segment length for the current problem would be less than 0.125mm long. Columns 3-6 therefore chart the convergence of the 'precise' frequencies to their exact counterparts in column 7, with increasing *M*. It should be noted that the 'precise' results of column 6 are identical to the exact Timoshenko results of column 7, which were determined from a general computer program based on Eq.(8) and using exact member theory [12,13]. Columns 8 and 9 give the lower (first spectrum) and upper (second spectrum) frequencies satisfying Eqs.(12), but now written in ascending order and retained in their respective columns for comparison. The table is rounded off by columns 10 and 11, which note the values of Φ and Λ for each of the first and second spectrum frequencies, respectively. This confirms that all first and second spectrum frequencies correspond to integer multiples of π and that the values in columns 8 and 9 also satisfy Eqs.(16). Table 3 is important because it shows beyond all doubt that the 'precise' model, which cannot have a second spectrum, yields results for sufficiently large *M*, that match identically with the exact Timoshenko results from any of the sources described in the paper, when written in ascending order. Furthermore, if the results of the precise approach given in column 6, which comprise a single continuous spectrum, are now taken as the datum, there is no indication, to the accuracy of the results presented, that the inherent accuracy of second spectrum frequencies is any different to that of the first spectrum, as has been suggested elsewhere [8].

Table 4 identifies the modal type associated with each of the fifteen frequencies identified in Table 3 according to the procedure described in Section 2.3.1., which clearly parallels the data of Table 3. Thus it can be gleaned from either table, that the frequency/mode sequencing does not adhere to a fixed pattern and hence that, in any analysis, it will always be beneficial to be in a position to define frequency/modal provenance.

Table 5 gives numerical values of the mode shape corresponding to the cut-off frequency, together with a selection of typical first and second spectrum flexural modes, taken across the load categories and which occur predominantly around the cut-of frequency or at higher frequencies. In each case the mode has been scaled by the absolute value of its largest element. It is interesting to note that on close comparison between mode $(p^2 = 0,\ \Phi_5)$ and mode $(p^2 < 0,\ \Phi_5)$ there is very little difference between them, thus confirming that an axial load has little effect on such squat members at high frequencies. Although not shown, this pattern is typical across all modes in Table 4 with the same *m* value and likewise with all modes with the same *n* value.

The flexural mode shapes given in Table 5 are also reproduced in diagrammatic form in Fig. 1. In this case, each mode shape was constructed by calculating a scale factor for the lateral displacement by dividing the reciprocal of the logarithm of peak rotational displacement by peak lateral displacement. This has the effect of amplifying smaller displacements to make them visually identifiable while imposing negligible effects on the larger values. This is particularly helpful in the case of second spectrum (Λ_n) modes, where it can be shown that the lateral displacements are particularly small over a wide range of frequencies [15]. Fig. 2 highlights the important difference that exists between corresponding first and second spectrum modes in which $m = n$. In the first pair, $m = n = 1$, $p^2 < 0$ and

the lateral displacement is symmetric about the mid-length of the member, while in the second pair $m = n = 2$, $p^2 < 0$ and the lateral displacement is anti-symmetric. The difference between the modes in each pair is clear, thus confirming their mutual independence, as discussed in Section 2.3.1.

Table 6 presents the results determined from the 'precise' approach for $M = 12$ when the distributed rotary inertia of the member is scaled by the factors shown. Factors of zero and one therefore yield the results for Eqs.(11) and (8), in columns 2 and 12, respectively. The intermediate values then indicate a smooth and monotonic transition between the two. This shows that there is a unique, one-to-one correspondence between each B-E frequency and its Timoshenko counterpart, which most importantly includes the cut-off frequency. Furthermore, the modal number of the B-E frequency that maps to the cut-off frequency can be determined *a priori* from the problem data, as follows. Eqs.(14) define the cut-off frequency. Thus, substituting these in Eq.(16a) and noting that the cut-off frequency corresponds to the first value of Φ that is not an integer multiple of π, the required modal number is given by

$$\text{the smallest integer} > [(r^2 + s^2)/(1 - s^2 p^2)]^{1/2} / rs\pi \tag{21}$$

which can be tested easily using the current data and results.

These facts, together with the fact that Timoshenko theory provides infinitely close bounds on the cut-off frequency, provide a compelling argument that the cut-off frequency should be thought of as a true Timoshenko frequency.

Table 7 gives the non-dimensional frequency parameters, b_i, from the 'precise' approach with $M = 12$, for a variety of foundation stiffness combinations. The distributed foundation stiffnesses are additionally incorporated into the original 'precise' model by adding equivalent lumped stiffnesses into the appropriate locations of the datum segment stiffness matrix. The table shows that; the cut-off frequency remains unchanged when $k_\theta = 0$ and rises otherwise; there are no additional frequencies as a consequence of the term $\left(b_i^2 - k_y^*\right) = 0$ and that the effect of a distributed rotational foundation stiffness is greater than that of its lateral counterpart.

5. Conclusions

The main conclusions that can be deduced from the body of the paper are set out below. Initially, however, it is useful to consider two generic areas of note.

Firstly, the general equations presented allow for any combination of second order effects, including static axial load. Traditionally, this latter option has rarely been considered in Timoshenko theory, despite the fact that it often influences the lower frequencies, creates no anomalies and offers a more complete description of the problem.

Secondly, the addition of a distributed elastic foundation generates an intractable problem from which exact solutions are difficult to obtain. One exception to this is a simple formula that shows how the rotational component of foundation stiffness uniquely raises the cut-off frequency, while retaining its identity as a pure shear mode. On the other hand, the ability to provide general solutions to such problems has been achieved through the use of a simple and extremely efficient 'precise' approach that has been shown to offer excellent accuracy.

The remaining conclusions assume the absence of a distributed foundation, but are unaffected by whether or not a static axial load is present in the member. In the first of these, it has been shown that both spectra of Timoshenko frequencies can be determined from the single quadratic equation governing their exact solution. This classical problem is easily solved, but fails to determine the cut-off frequency, since it corresponds to a singularity in the equation at that point. However, this is easily remedied by use of a simple, exact formula or, conversely, the value can be converged upon to any desired accuracy, since the theory is valid at infinitely close lower and upper bounds. The modal vectors corresponding to all such frequencies are easy to obtain by conventional methods, such as forward elimination and backward substitution of the stiffness equations in the present case. A typical selection are presented, both in numerical and graphic form, with particular attention given to confirming the necessary independence of the second spectrum modes.

The complete range of exact Timoshenko frequencies, described in the paragraph above, can also be generated using the 'precise' technique, when programmed to emulate Timoshenko theory. In this form, it generates a single spectrum of frequencies that, to the accuracy of presentation, match identically the exact Timoshenko frequencies, including the cut-off frequency. When this is linked to the following facts, namely: that one frequency from the continuous B-E spectrum, whose modal value can be identified *a priori* from the problem data, maps exactly to the cut-off frequency; that all remaining B-E frequencies each map uniquely to a single Timoshenko frequency in either the first or second spectrum; that any theory which seeks to improve accuracy must do so without loss or gain of any frequencies; it is our conjecture that all frequencies in the first and second spectra, together with the cut-off frequency, comprise the single spectrum of Timoshenko frequencies.

References

[1] S.P. Timoshenko. On the correction for shear of the differential equation for transverse vibration of prismatic bars. Philosophical Magazine 41 (1921) 744–746.
[2] B.A.H Abbas, J. Thomas. The second frequency spectrum of Timoshenko beams. Journal of Sound and Vibration 51 (1977) 123–137.
[3] G.R. Bhashyam, G. Prathap. The second frequency spectrum of Timoshenko beams. Journal of Sound and Vibration 76 (1981) 407–420
[4] N.G. Stephen. The second frequency spectrum of Timoshenko beams. Journal of Sound and Vibration 80 (1982) 578–582.
[5] M. Levinson, D.W. Cooke. On the two frequency spectra of Timoshenko beams. Journal of Sound and Vibration 84 (1982) 319–326.
[6]G. Prathap. The two frequency spectra of Timoshenko beams – a re-assessment. Journal of Sound and Vibration 90 (1983) 443–445. See also M. Levinson, Author's Reply 445-446.
[7] S. Ekwaro-Osire, D.H.S Maithripala, J.M. Berg. A series expansion approach to interpreting the spectra of the Timoshenko beam. Journal of Sound and Vibration 240 (2001) 667–678.
[8] N.G. Stephen. The second spectrum of Timoshenko beam theory—further assessment. Journal of Sound and Vibration 292 (2006) 372–389.
[9] N.G. Stephen, S. Puchegger. On the valid frequency range of Timoshenko beam theory. Journal of Sound and Vibration 297 (2006) 1082–1087.
[10] W.H. Wittrick, F.W.Williams. A general algorithm for computing natural frequencies of elastic structures. Quarterly Journal Mechanics Applied Mathematics 24 (1971) 263–284.
[11] M.D. Capron, F. W. Williams. Exact dynamic stiffnesses for an axially loaded uniform Timoshenko member embedded in an elastic medium. Journal of Sound and Vibration 412 (1988) 453-466.
[12] W.P. Howson, F. W. Williams. Natural frequencies of frames with axially loaded Timoshenko members. Journal of Sound and Vibration 26 (1973) 503-515.
[13] W.P. Howson, J.R. Banerjee, F.W. Williams. Concise equations and program for exact eigensolutions of plane frames including member shear. Advances in Engineering Software 5 (1983) 137-141.
[14] C.T. Hopper and F.W. Williams. Mode finding in nonlinear structural eigenvalue calculations. Journal of Structural Mechanics 5 (1977) 255-278.
[15] A.I. Manevich. Dynamics of Timoshenko beam on linear and nonlinear foundation: Phase relations, significance of the second spectrum, stability. Journal of Sound and Vibration 344 (2015) 209-220.
[16] F.W. Williams, D. Kennedy, M.S. Djoudi. The member stiffness determinant and its uses for the transcendental eigenproblems of structural engineering and other disciplines. Proceedings of The Royal Society A: Mathematical, Physical and Engineering Sciences 459 (2003) 1001-1019.
[17] Q. Gao, Z. Wanxie, W.P. Howson. A precise method for solving wave propagation problems in layered anisotropic media. Wave Motion 40 (2004) 191-207.
[18] N. El-Kaabazi, D. Kennedy. Calculation of natural frequencies and vibration modes of variable thickness cylindrical shells using the Wittrick-Williams algorithm. Computers & Structures 104-5 (2012) 4-12.

Appendix *Some simple physical relationships*

The uniform beam shown in Fig. A1 (a) and (b) is symmetric about its mid-length. Therefore the modes of vibration in each case may be divided into a set that is symmetric about the mid-length, which may be found, respectively, from the half members of Fig. A2 (aS) and (bS), and an anti-symmetric set given by the half members of Fig. A2 (aA) and (bA).

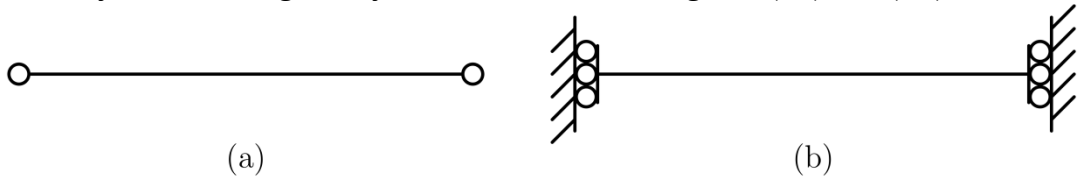

Fig. A1. Two alternative sets of boundary conditions of a uniform beam of length L. The hinged-hinged supports of (a) allow rotation, but prevent displacement, while those of (b) allow precisely the opposite.

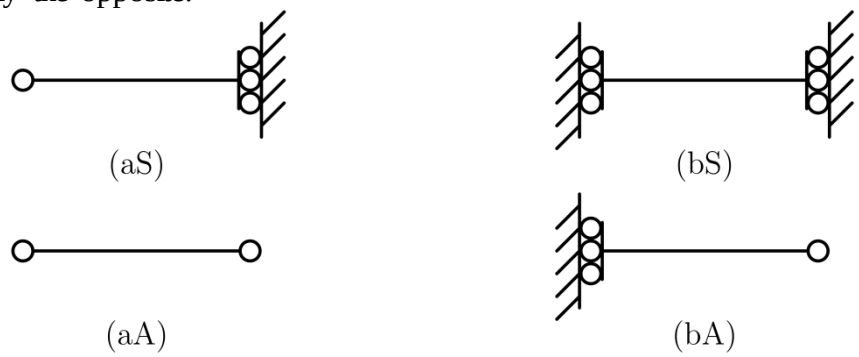

Fig. A2. Half members used to find the symmetric (S) and anti-symmetric (A) modes of the beam of Fig. A1.

Fig. A2 (aS) and (bA) clearly both define the same physical problem and therefore give the same natural frequencies. Equally clearly, Fig. A2 (aA) and (bS) are related to each other in exactly the same way as the two cases of Fig. A1 (a) and (b). Hence the argument used to obtain Fig. A2 from Fig. A1, and the associated deductions given above, can be applied recursively until the members of Fig. A2 are of infinitesimal length. Thus it follows that all natural frequencies for the case of Fig. A1 (a) are identical to those of Fig. A1 (b), except that the former has any natural frequencies possessed by an infinitesimally short beam of the type shown in Fig. A2 (aA), whereas the latter has any natural frequencies possessed by an infinitesimally short beam of the type shown in Fig. A2 (bS). This accounts for the fact that the beam of Fig. A1 (a) does not have a rigid body mode, while that of Fig. A1 (b) does.

In the physical argument used above, it is only assumed that the member is uniform. The arguments must therefore apply to any member with any uniform combination of member properties, second order effects and other externally imposed conditions, such as distributed foundations.

The corollary to the above, is that a uniform member of length, L, with hinged-guided boundary conditions will have all the natural frequencies corresponding to either the symmetric modes of a hinged-hinged beam or the anti-symmetric modes of a guided-guided beam, of length $2L$ in each case.

The conclusions that can be drawn from the above are:

1. that the non-zero frequencies of a guided-guided beam are identical to those of a hinged-hinged beam; and

2. the frequencies stemming from a beam with any combination of the above boundary conditions, can always be found from a beam in which the frequency equation factorises.

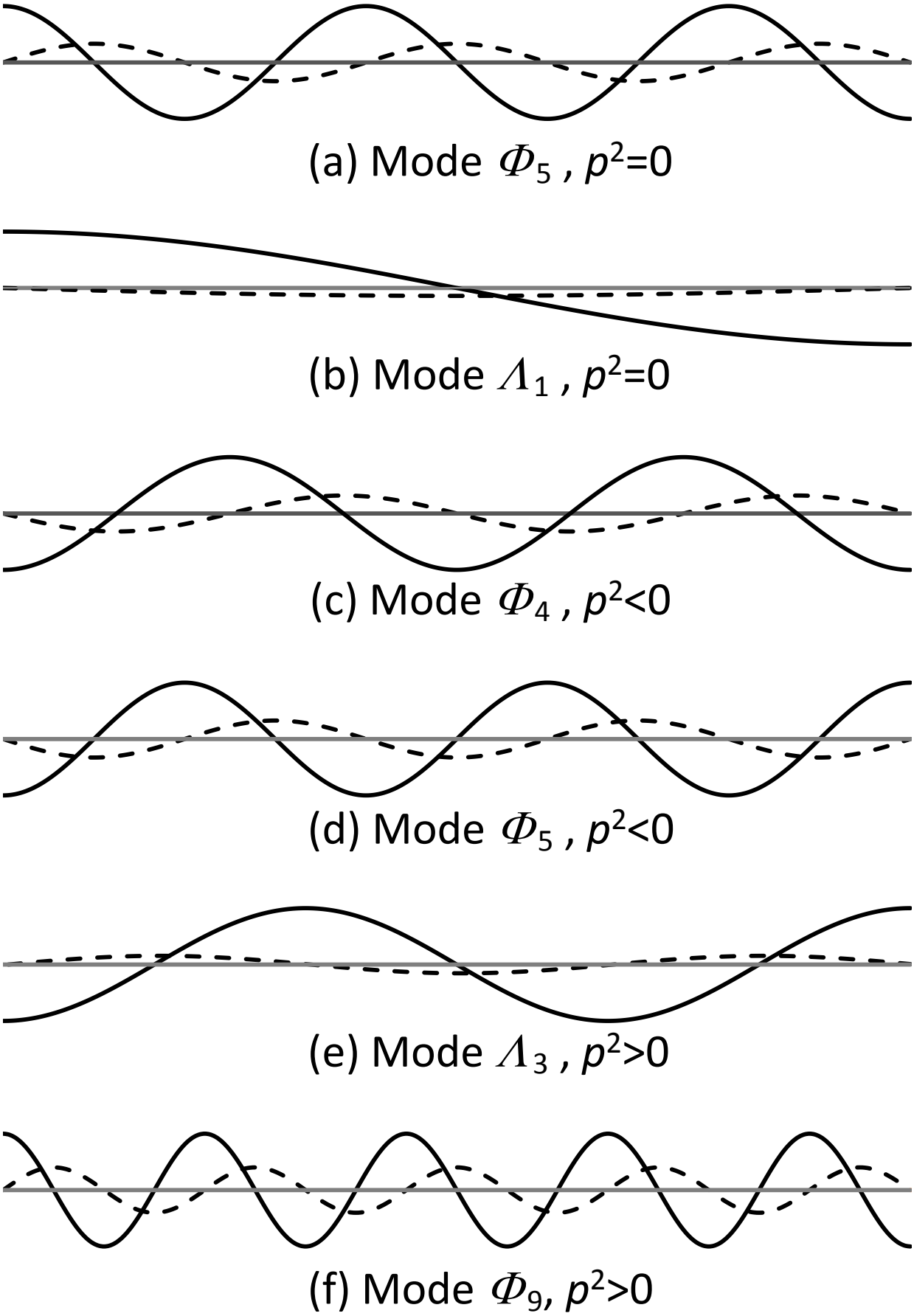

Fig. 1. Diagrammatic representation of the flexural mode shapes given in Table 5. The dashed and solid lines represent lateral displacement and bending slope respectively.

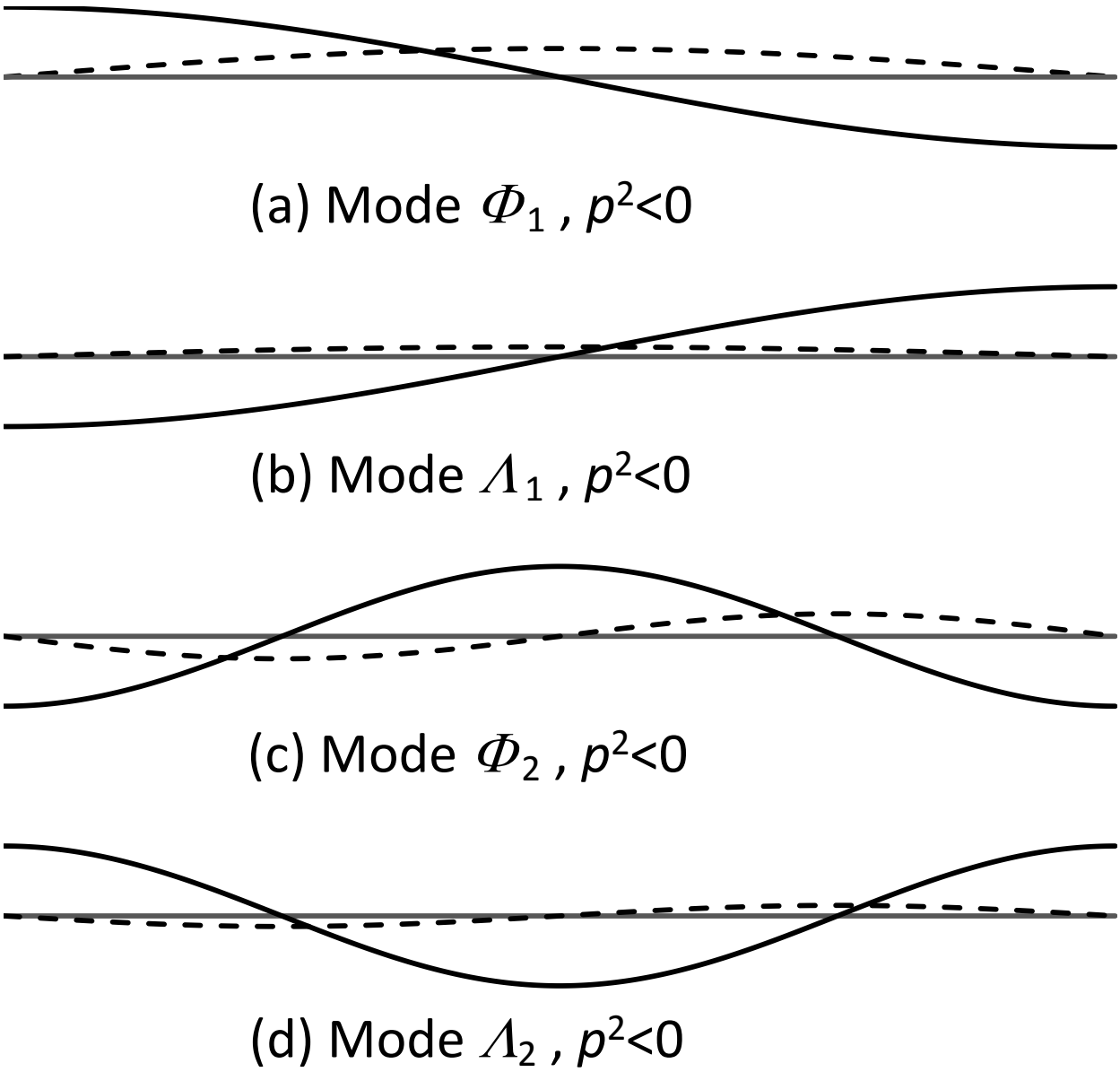

Fig. 2. Comparison of modes ($p^2 < 0,\ \Phi_1,\ \Lambda_1$) and modes ($p^2 < 0,\ \Phi_2,\ \Lambda_2$) in order to illustrate the independence of second spectrum modes with respect to their first spectrum counterparts.

Table 1

Exact non-dimensional frequency parameters, b_i, stemming from Eq.(11) with $s^2 = 0$ (columns 2, 4 and 6) and $s^2 \neq 0$ (columns 3, 5 and 7). These results are for the data given in Section 3 and it should be noted that $b_{p,i} = b_{0,i}$ when $p^2 = 0$ *etc*.

1	2	3	4	5	6	7
i	$b_{p,i}$	$b_{ps,i}$	$b_{p,i}$	$b_{ps,i}$	$b_{p,i}$	$b_{ps,i}$
	$p^2 = 0$		$p^2 < 0$		$p^2 > 0$	
1	9.86960	9.18664	12.0887	11.5379	6.97721	5.97217
2	39.4784	31.0474	41.8743	34.0419	36.9274	27.7314
3	88.8264	57.4822	91.2616	61.1780	86.3226	53.5318
4	157.914	84.8043	160.363	89.2827	155.426	80.0757
5	246.740	111.978	249.196	117.291	244.259	106.399
6	355.306	138.812	357.766	144.993	352.829	132.343
7	483.611	165.329	486.073	172.399	481.136	157.943
8	631.655	191.590	634.118	199.563	629.181	183.271
9	799.438	217.650	801.903	226.536	796.966	208.386
10	986.960	243.555	989.426	253.361	984.489	233.337
11	1194.22	269.337	1196.69	280.069	1191.75	258.160
12	1421.22	295.023	1423.69	306.685	1418.75	282.882
13	1667.96	320.632	1670.43	333.227	1665.49	307.522
14	1934.44	346.178	1936.91	359.708	1931.97	332.098
15	2220.66	371.673	2223.13	386.141	2218.19	356.619

Table 2

Exact, non-dimensional, Timoshenko frequency parameters, b_i, corresponding to the lower, $b_{L,i}$, and upper, $b_{U,i}$, solutions of Eq.(10), which are calculated from Eqs.(12) using the data given in Section 3.

1	2	3	4	5	6	7
i	$b_{L,i}$	$b_{U,i}$	$b_{L,i}$	$b_{U,i}$	$b_{L,i}$	$b_{U,i}$
	$p^2 = 0$		$p^2 < 0$		$p^2 > 0$	
1	9.01341	121.381	11.3196	121.389	5.85991	121.374
2	29.8430	146.642	32.7095	146.695	26.6651	146.590
3	55.0459	178.879	58.5478	178.992	51.2947	178.768
4	81.5627	214.619	85.8052	214.781	77.0711	214.463
5	108.361	252.411	113.416	252.603	103.038	252.227
6	135.097	291.539	141.012	291.746	128.888	291.342
7	161.670	331.595	168.475	331.807	154.541	331.394
8	188.062	372.323	195.777	372.534	179.992	372.123
9	214.287	413.552	222.924	413.758	205.262	413.358
10	240.366	455.164	249.934	455.363	230.377	454.977
11	266.321	497.074	276.826	497.265	255.361	496.894
12	292.171	539.219	303.617	539.402	280.236	539.047
13	317.934	581.553	330.323	581.728	305.021	581.390
14	343.623	624.042	356.958	624.209	329.729	623.886
15	369.250	666.657	383.531	666.817	354.373	666.508

Table 3

The non-dimensional frequency parameters, b_i, given by the 'precise' approach for various values of M, are compared with those from relevant equations in the body of the paper, together with illustrative supporting results. b_{co} is the cut-off frequency and the data are those given in Section 3.

1	2	3	4	5	6	7	8	9	10	11
i	$b_{ps,i}$		b_i from 'precise' with M =			Exact solution of	$b_{L,i}$ ($b_{\Phi,i}$)	$b_{U,i}$ ($b_{\Lambda,i}$)	Φ	Λ
	Eq.(11)	3	5	8	12	Eq.(8)	Eq.(12a) Eq.(16a)	Eq.(12b) Eq.(16b)	Eq.(17a)	Eq.(17b)
					$p^2 = 0$					
1	9.18664	9.01332	9.01341	9.01341	9.01341	9.01341	9.01341		3.14159	
2	31.0474	29.8355	29.8425	29.8430	29.8430	29.8430	29.8430		6.28319	
3	57.4822	54.9890	55.0426	55.0458	55.0459	55.0459	55.0459		9.42478	
4	84.8043	81.3692	81.5525	81.5626	81.5627	81.5627	81.5627		12.5664	
5	111.978	106.498	108.339	108.360	108.361	108.361	108.361		15.7080	
6	138.812	107.898	110.564	110.847	110.851	110.851	$\boldsymbol{b_{co} = 110.851}$		16.0000	
7	165.329	115.888	121.018	121.375	121.381	121.381		121.381	17.2359	3.14159
8	191.590	134.144	135.061	135.097	135.097	135.097	135.097		18.8496	4.99281
9	217.650	137.414	146.029	146.632	146.642	146.642		146.642	20.2119	6.28319
10	243.555	159.687	161.616	161.669	161.670	161.670	161.670		21.9911	7.80459
11	269.337	162.458	177.782	178.861	178.879	178.879		178.879	24.0372	9.42478
12	295.023	179.344	187.989	188.061	188.062	188.062	188.062		25.1327	10.2549
13	320.632	186.333	212.719	214.285	214.287	214.287	214.287		28.2743	12.5381
14	346.178	205.965	214.193	214.589	214.619	214.619		214.619	28.3143	12.5664
15	371.673	208.340	240.250	240.364	240.366	240.366	240.366		31.4159	14.7207
					$p^2 < 0$					
1	11.5379	11.3194	11.3196	11.3196	11.3196	11.3196	11.3196		3.14159	
2	34.0419	32.6995	32.7089	32.7094	32.7095	32.7095	32.7095		6.28319	
3	61.1780	58.4774	58.5438	58.5477	58.5478	58.5478	58.5478		9.42478	
4	89.2827	85.5705	85.7929	85.8050	85.8052	85.8052	85.8052		12.5664	
5	117.291	106.503	110.564	110.847	110.851	110.851	$\boldsymbol{b_{co} = 110.851}$		15.4164	
6	144.993	112.856	113.391	113.416	113.416	113.416	113.416		15.7080	1.50519
7	172.399	115.903	121.025	121.383	121.389	121.389		121.389	16.6145	3.14159
8	199.563	137.486	140.969	141.012	141.012	141.012	141.012		18.8496	5.66742
9	226.536	139.850	146.083	146.686	146.695	146.695		146.695	19.4982	6.28319
10	253.361	162.625	168.411	168.474	168.475	168.475	168.475		21.9911	8.44825
11	280.069	166.011	177.897	178.975	178.992	178.992		178.992	23.1992	9.42478
12	306.685	185.449	195.690	195.775	195.777	195.777	195.777		25.1327	10.9262
13	333.227	186.641	212.884	214.752	214.781	214.781		214.781	27.3303	12.5664
14	359.708	206.609	222.812	222.922	222.924	222.924	222.924		28.2743	13.2545
15	386.141	214.708	249.488	249.932	249.934	249.934	249.934		31.4159	15.4903
					$p^2 > 0$					
1	5.97217	5.85989	5.85991	5.85991	5.85991	5.85991	5.85991		3.14159	
2	27.7314	26.6599	26.6648	26.6651	26.6651	26.6651	26.6651		6.28319	
3	53.5318	51.2500	51.2921	51.2947	51.2947	51.2947	51.2947		9.42478	
4	80.0757	76.9142	77.0628	77.0710	77.0711	77.0711	77.0711		12.5664	
5	106.399	102.660	103.020	103.037	103.038	103.038	103.038		15.7080	
6	132.343	106.491	110.564	110.847	110.851	110.851	$\boldsymbol{b_{co} = 110.851}$		16.6553	
7	157.943	115.871	121.010	121.368	121.374	121.374		121.374	17.9340	3.14159
8	183.271	128.114	128.858	128.888	128.888	128.888	128.888		18.8496	4.22236
9	208.386	137.340	145.977	146.580	146.590	146.590		146.590	21.0147	6.28319
10	233.337	152.956	154.497	154.540	154.541	154.541	154.541		21.9911	7.10596
11	258.160	162.288	177.670	178.750	178.768	178.768		178.768	24.9811	9.42478
12	282.882	172.640	179.932	179.991	179.992	179.992	179.992		25.1327	9.53681
13	307.522	186.007	205.185	205.261	205.262	205.262	205.262		28.2743	11.7771
14	332.098	200.999	212.560	214.433	214.463	214.463		214.463	29.4232	12.5664
15	356.619	205.192	230.281	230.375	230.377	230.377	230.377		31.4159	13.9070

Table 4

Modal identification for the fifteen exact frequencies of the hinged-hinged Timoshenko beam for each load category, as set out in Table 3. **S** signifies the Shear mode, while *m* and *n* denote the flexural mode numbers corresponding to those frequencies stemming from the first and second spectrum, respectively.

	Modal No., *i* in Table 3	1	2	3	4	5	6	7	8	9	10	11	12	13	14	15
$p^2=0$	Flexural Modal No. m (Φ_m)	1	2	3	4	5			6		7		8	9		10
							S									
	Flexural Modal No. n (Λ_n)							1		2		3			4	
$p^2<0$	Flexural Modal No. m (Φ_m)	1	2	3	4		5		6		7		8		9	10
						S										
	Flexural Modal No. n (Λ_n)							1		2		3		4		
$p^2>0$	Flexural Modal No. m (Φ_m)	1	2	3	4	5			6		7		8	9		10
							S									
	Flexural Modal No. n (Λ_n)							1		2		3			4	

Table 5

Numerical examples for a selection of typical, normalised mode shapes that can be identified by their i or b values (Table 3) or their m or n values (Table 4). V_ξ, Υ_ξ and Ψ_ξ are the amplitudes of the lateral displacement, shear slope and bending slope, respectively, at a distance ξ from the left hand end of the member.

			$p^2=0$				$p^2<0$				$p^2>0$			
	b_{co}=110.851		b=108.361		b=121.381		b=85.8052		b=113.416		b=178.768		b=205.262	
	Shear Mode $p^2=0$, $p^2<0$ $p^2>0$		i=5, m=5 (Φ_5)		i=7, n=1 (Λ_1)		i=4, m=4 (Φ_4)		i=6, m=5 (Φ_5)		i=11, n=3 (Λ_3)		i=13, m=9 (Φ_9)	
$\xi=x/L$	V_ξ	Υ_ξ	V_ξ	Ψ_ξ	V_ξ	Ψ_ξ	V_ξ	Ψ_ξ	V_ξ	Ψ_ξ	V_ξ	Ψ_ξ	V_ξ	Ψ_ξ
0.0	0.000	-1.000	0.000	-1.000	0.000	-1.000	0.000	1.000	0.000	1.000	0.000	1.000	0.000	-1.000
0.1	0.000	-1.000	-0.124	0.000	0.002	-0.951	0.109	0.309	0.121	0.000	-0.009	0.588	-0.055	0.951
0.2	0.000	-1.000	0.000	1.000	0.004	-0.809	0.067	-0.809	0.000	-1.000	-0.011	-0.309	0.105	-0.809
0.3	0.000	-1.000	0.124	0.000	0.006	-0.588	-0.067	-0.809	-0.121	0.000	-0.003	-0.951	-0.144	0.588
0.4	0.000	-1.000	0.000	-1.000	0.007	-0.309	-0.109	0.309	0.000	1.000	0.007	-0.809	0.169	-0.309
0.5	0.000	-1.000	-0.124	0.000	0.007	0.000	0.000	1.000	0.121	0.000	0.011	0.000	-0.178	0.000
0.6	0.000	-1.000	0.000	1.000	0.007	0.309	0.109	0.309	0.000	-1.000	0.007	0.809	0.169	0.309
0.7	0.000	-1.000	0.124	0.000	0.006	0.588	0.067	-0.809	-0.121	0.000	-0.003	0.951	-0.144	-0.588
0.8	0.000	-1.000	0.000	-1.000	0.004	0.809	-0.067	-0.809	0.000	1.000	-0.011	0.309	0.105	0.809
0.9	0.000	-1.000	-0.124	0.000	0.002	0.951	-0.109	0.309	0.121	0.000	-0.009	-0.588	-0.055	-0.951
1.0	0.000	-1.000	0.000	1.000	0.000	1.000	0.000	1.000	0.000	-1.000	0.000	-1.000	0.000	1.000

Table 6

Non-dimensional frequency parameters, b_i, from the 'precise' approach with M = 12 when the distributed rotary inertia is scaled by the factors shown. The data are those given in Section 3.

1	2	3	4	5	6	7	8	9	10	11	12
i	Eq.(11)										Eq.(8)
					Precise with M = 12 and distributed rotary inertia factor =						
	0.0	0.1	0.2	0.3	0.4	0.5	0.6	0.7	0.8	0.9	1.0
						$p^2 = 0$					
1	9.18664	9.16896	9.15136	9.13384	9.11640	9.09903	9.08175	9.06455	9.04743	9.03038	9.01341
2	31.0474	30.9254	30.8037	30.6823	30.5613	30.4406	30.3202	30.2003	30.0807	29.9616	29.8430
3	57.4822	57.2478	57.0111	56.7721	56.5310	56.2879	56.0429	55.7961	55.5475	55.2974	55.0459
4	84.8043	84.5108	84.2105	83.9032	83.5892	83.2682	82.9405	82.6060	82.2647	81.9170	81.5627
5	111.978	111.667	111.346	111.014	110.671	110.316	109.949	109.571	109.180	108.777	108.361
6	138.812	138.506	138.188	137.856	137.510	137.148	136.772	132.493	123.935	116.847	110.851
7	165.329	165.038	164.733	164.412	164.076	156.767	143.108	136.379	135.198	127.706	121.381
8	191.590	191.316	191.028	190.724	175.271	163.723	155.523	144.260	135.969	135.542	135.097
9	217.650	217.394	217.124	202.386	189.752	170.043	163.352	162.963	162.553	153.962	146.642
10	243.555	243.316	243.063	216.839	190.404	190.066	186.334	173.197	162.655	162.122	161.670
11	269.337	269.114	247.871	218.689	216.536	203.312	189.709	189.331	188.932	187.697	178.879
12	295.023	294.814	267.325	242.795	226.412	216.216	215.875	210.926	198.186	188.509	188.062
13	320.632	320.436	268.877	260.406	242.510	242.208	226.823	215.514	215.130	214.722	214.287
14	346.178	345.994	294.593	268.626	268.358	247.390	241.886	241.543	237.904	225.250	214.619
15	371.673	350.542	317.674	294.356	275.401	268.073	267.769	253.279	241.176	240.785	240.366
						$p^2 < 0$					
1	11.5379	11.5156	11.4935	11.4715	11.4495	11.4276	11.4059	11.3842	11.3625	11.3410	11.3196
2	34.0419	33.9080	33.7742	33.6405	33.5069	33.3734	33.2401	33.1071	32.9743	32.8417	32.7095
3	61.1780	60.9282	60.6751	60.4189	60.1597	59.8976	59.6327	59.3651	59.0950	58.8225	58.5478
4	89.2827	88.9732	88.6552	88.3288	87.9939	87.6504	87.2983	86.9377	86.5686	86.1910	85.8052
5	117.291	116.965	116.627	116.275	115.910	115.532	115.138	114.731	114.308	113.870	110.851
6	144.993	144.673	144.338	143.987	143.620	143.235	142.831	132.493	123.935	116.847	113.416
7	172.399	172.095	171.774	171.436	171.079	156.767	143.108	142.408	135.203	127.713	121.389
8	199.563	199.277	198.975	198.654	175.271	170.046	155.527	144.264	141.964	141.499	141.012
9	226.536	226.269	225.986	202.386	189.754	170.703	170.306	169.885	162.693	154.008	146.695
10	253.361	253.112	247.871	218.690	198.315	197.954	186.359	173.228	169.441	168.972	168.475
11	280.069	279.836	252.847	225.685	225.364	203.331	197.571	197.164	196.731	187.793	178.992
12	306.685	306.467	267.326	252.564	226.425	225.022	224.658	210.991	198.266	196.269	195.777
13	333.227	333.022	279.588	260.415	252.263	247.429	226.874	224.268	223.851	223.404	214.781
14	359.708	350.542	306.235	279.323	275.429	251.940	251.595	251.224	238.015	225.386	222.924
15	386.141	359.516	317.679	305.986	279.040	278.736	272.539	253.369	250.825	250.396	249.934
						$p^2 > 0$					
1	5.97217	5.96067	5.94924	5.93787	5.92656	5.91531	5.90411	5.89298	5.88190	5.87088	5.85991
2	27.7314	27.6225	27.5142	27.4062	27.2988	27.1919	27.0855	26.9796	26.8742	26.7694	26.6651
3	53.5318	53.3138	53.0943	52.8734	52.6512	52.4277	52.2030	51.9773	51.7506	51.5230	51.2947
4	80.0757	79.7991	79.5171	79.2296	78.9368	78.6387	78.3353	78.0268	77.7132	77.3945	77.0711
5	106.399	106.105	105.802	105.489	105.168	104.837	104.497	104.147	103.787	103.417	103.038
6	132.343	132.052	131.750	131.437	131.112	130.775	130.425	130.062	123.935	116.847	110.851
7	157.943	157.666	157.376	157.074	156.758	156.428	143.108	132.493	129.685	127.700	121.374
8	183.271	183.010	182.736	182.449	175.271	156.767	155.520	144.255	135.193	129.294	128.888
9	208.386	208.142	207.885	202.386	182.148	170.041	156.083	155.723	155.346	153.917	146.590
10	233.337	233.109	232.868	207.615	189.750	181.832	181.500	173.166	162.617	154.953	154.541
11	258.160	257.947	247.871	218.687	207.330	203.293	186.309	181.151	180.784	180.398	178.768
12	282.882	282.682	257.721	232.615	226.398	207.031	206.715	206.381	198.107	187.602	179.992
13	307.522	307.335	267.324	257.483	232.347	232.064	226.772	210.862	206.029	205.656	205.262
14	332.098	331.921	282.471	260.397	257.232	247.352	231.765	231.448	231.112	225.119	214.463
15	356.619	350.542	307.136	282.247	275.374	256.965	256.682	253.192	237.796	230.755	230.377

Table 7

Non dimensional frequency parameters, b_i, from the 'precise' approach with M = 12 and the data given in Section 3, for a selection of two parameter foundations. The values in bold type correspond to the cut-off frequencies and the units of k_θ and k_y are N and Nm^{-2} respectively.

1	2	3	4	5	6	7	8	9	10	11
	$k_\theta = 0$		$k_\theta = 0$			$k_y = 0$				
i	$k_y = 0$		$k_y =$			$k_\theta =$			$k_\theta = k_y =$	
		10^6	10^8	10^{10}	10^6	10^8	10^{10}	10^6	10^8	10^{10}
					$p^2 = 0$					
1	9.01341	9.01351	9.02317	9.94181	9.01634	9.29886	18.7933	9.01644	9.30833	19.2689
2	29.8430	29.8430	29.8458	30.1237	29.8448	30.0280	39.5820	29.8449	30.0308	39.8057
3	55.0459	55.0459	55.0474	55.1965	55.0470	55.1621	62.5707	55.0471	55.1636	62.7104
4	81.5627	81.5627	81.5637	81.6649	81.5635	81.6379	87.0397	81.5635	81.6389	87.1394
5	108.361	108.361	108.361	108.438	108.361	108.411	112.317	108.361	108.412	112.394
6	**110.851**	**110.851**	**110.851**	**110.851**	**110.858**	**111.483**	137.982	**110.858**	**111.483**	138.046
7	121.381	121.381	121.381	121.384	121.387	121.937	**162.270**	121.387	121.937	**162.270**
8	135.097	135.097	135.098	135.160	135.098	135.132	163.807	135.098	135.133	163.861
9	146.642	146.642	146.642	146.647	146.646	147.082	168.834	146.646	147.082	168.834
10	161.670	161.670	161.670	161.723	161.670	161.695	186.738	161.670	161.695	186.740
11	178.879	178.878	178.879	178.883	178.882	179.235	189.674	178.882	179.235	189.720
12	188.062	188.062	188.062	188.108	188.062	188.080	212.499	188.062	188.081	212.501
13	214.287	214.287	214.287	214.328	214.287	214.300	215.523	214.287	214.301	215.564
14	214.619	214.619	214.619	214.623	214.622	214.918	241.330	214.622	214.918	241.367
15	240.366	240.366	240.366	240.402	240.366	240.376	243.272	240.366	240.377	243.274
					$p^2 < 0$					
1	11.3196	11.3197	11.3274	12.0717	11.3219	11.5496	20.0358	11.3220	11.5572	20.4826
2	32.7095	32.7095	32.7120	32.9654	32.7112	32.8813	41.9047	32.7112	32.8839	42.1159
3	58.5478	58.5478	58.5492	58.6892	58.5489	58.6602	65.8379	58.5489	58.6616	65.9705
4	85.8052	85.8052	85.8062	85.9020	85.8059	85.8793	91.1962	85.8060	85.8803	91.2913
5	**110.851**	**110.851**	**110.851**	**110.851**	**110.858**	**111.483**	117.354	**110.858**	**111.483**	117.428
6	113.416	113.416	113.417	113.490	113.417	113.466	143.908	113.417	113.467	143.969
7	121.389	121.389	121.389	121.392	121.394	121.944	**162.270**	121.394	121.944	**162.270**
8	141.012	141.012	141.013	141.073	141.013	141.048	168.835	141.013	141.048	168.836
9	146.695	146.695	146.695	146.700	146.700	147.135	170.634	146.700	147.135	170.686
10	168.475	168.475	168.476	168.526	168.475	168.500	186.753	168.475	168.501	186.755
11	178.992	178.992	178.992	178.997	178.996	179.348	197.413	178.996	179.348	197.457
12	195.777	195.777	195.777	195.821	195.777	195.795	212.544	195.777	195.796	212.546
13	214.781	214.781	214.781	214.785	214.784	215.078	224.184	214.784	215.078	224.224
14	222.924	222.924	222.924	222.963	222.924	222.938	243.352	222.924	222.938	243.354
15	249.934	249.934	249.934	249.969	249.934	249.945	250.920	249.934	249.945	250.955
					$p^2 > 0$					
1	5.85991	5.86006	5.87491	7.20701	5.86438	6.28750	17.4626	5.86453	6.30149	17.9735
2	26.6651	26.6651	26.6683	26.9794	26.6672	26.8685	37.1134	26.6672	26.8716	37.3520
3	51.2947	51.2947	51.2963	51.4568	51.2959	51.4161	59.1200	51.2959	51.4177	59.2679
4	77.0711	77.0711	77.0722	77.1796	77.0719	77.1478	82.6676	77.0719	77.1489	82.7729
5	103.038	103.038	103.038	103.120	103.038	103.088	107.033	103.038	103.089	107.114
6	**110.851**	**110.851**	**110.851**	**110.851**	**110.858**	**111.483**	131.777	**110.858**	**111.483**	131.843
7	121.374	121.374	121.374	121.376	121.379	121.929	156.668	121.379	121.930	156.724
8	128.888	128.888	128.889	128.955	128.889	128.923	**162.270**	128.889	128.924	**162.270**
9	146.590	146.590	146.590	146.595	146.594	147.031	168.832	146.594	147.031	168.833
10	154.541	154.541	154.542	154.597	154.541	154.566	181.587	154.541	154.566	181.636
11	178.768	178.768	178.768	178.772	178.771	179.125	186.723	178.771	179.125	186.725
12	179.992	179.992	179.993	180.041	179.992	180.010	206.481	179.992	180.011	206.524
13	205.262	205.262	205.262	205.305	205.262	205.275	212.455	205.262	205.276	212.457
14	214.463	214.463	214.463	214.466	214.466	214.762	231.324	214.466	214.762	231.363
15	230.377	230.377	230.377	230.415	230.377	230.387	243.195	230.377	230.387	243.197